Seismo-acoustic wave propagation generated by the detonation of UXOs of large charge weights in a shallow water environment

Nathalie Favretto-Cristini, Anne Deschamps, David Ambrois, Mickaël Bonnin, Éric Beucler, E. Diego Mercerat, Fang Wang, Thierry Garlan, Xavier Demoulin, M. Arrigoni, et al.

PROCEEDINGS of the
24th International Congress on Acoustics

October 24 to 28, 2022, in Gyeongju, Korea

Extended abstract

Seismo-acoustic wave propagation generated by the detonation of UXOs of large charge weights in a shallow water environment

Nathalie FAVRETTO-CRISTINI[1]; Anne DESCHAMPS[2]; David AMBROIS[2]; Mickaël BONNIN[3]; Éric BEUCLER[3]; E. Diego MERCERAT[4]; Fang WANG[1,*]; Thierry GARLAN[5]; Xavier DEMOULIN[6]; Michel ARRIGONI[7]; Paul CRISTINI[1]; Olivier MORIO[5]; Romain SCHWAB[6,+]; Vadim MONTEILLER[1]

[1] Aix-Marseille Univ., CNRS, Centrale Marseille, LMA UMR 7031, Marseille, France

[2] Université Côte d'Azur, CNRS, Observatoire de la Côte d'Azur, IRD, Géoazur, Valbonne, France

[3] Nantes Université, Univ Angers, Le Mans Univ, CNRS, UMR6112, Laboratoire de Planétologie et Géosciences, Nantes, France

[4] Équipe REPSODY, CEREMA Méditerranée, Sophia-Antipolis, France

[5] Shom/DOPS/STM/SEDIM, Marine Geology Department, Brest, France

[6] MAREE, Plœmeur, France

[7] ENSTA Bretagne, Institut de Recherche Dupuy de Lôme, CNRS UMR 6027, Brest, France

[*] Now with CGG, Massy, France

[+] Now with ENSTA Bretagne, Lab-STICC, Brest, France

ABSTRACT

Unexploded historical ordnance (UXO) from World War II, that is discovered almost every week close to the French coast, must be destroyed quickly after discovery to ensure the safety of divers and ships. The favored destruction method is countermining, *i.e.*, the use of a high-order detonation conducted by exploding an additional donor charge placed adjacent to the UXO. In the framework of a UXO countermining campaign conducted in the Rade d'Hyères (Mediterranean Sea, France) in December 2018, hydro-acoustic and seismic recording systems have been deployed to record the explosion-induced waves in water and the seismic signals on the shore, respectively (POSA project). In this expanded abstract, we present the main observations and focus on the impact of the shallow water environment (whose water depth is less than 50 m), and more specifically on the impact of the unconsolidated sedimentary layer, on the recorded signals induced by the detonation of charges with weights ranging from 80 to 680 kg TNT-equivalent. We also discuss the acoustic-to-seismic wave conversions.

Keywords: Underwater explosion, wave propagation, seismo-acoustic signals

1. INTRODUCTION

Unexploded historical ordnance (UXO) from World War II are discovered almost every week close to the north-western and south-eastern coasts of metropolitan France. Quickly after their discovery, the French Navy Mine Warfare Office (FNMWO) must destroy the munitions to ensure the safety of divers and ships. The favored destruction method is countermining, *i.e.*, to use a high-order detonation conducted by exploding an additional donor charge placed adjacent to the UXO. Depending on whether the UXO is safe to move, such countermining occurs at specific safe locations or at the location of the discovery.

The risks for people in charge of the UXO countermining are well known by the FNMWO experts.

[1] favretto@lma.cnrs-mrs.fr

In contrast, it is difficult to reliably evaluate the possible consequences of underwater explosions on the marine environment and on the buildings located on the coast. Indeed, they depend mostly on the environment geology and on the characteristics (weight and location) of the explosive charges and, hence, on the detonation-induced wave propagation. Large underwater explosions may trigger small-scale landslides that could, in turn, generate large waves on the shore or damage infrastructures (pipelines, optic fibers). Therefore, there is a need for developing a decision support tool for the risk assessment regarding inland infrastructures before clearance of UXO of large weights.

One of the main goals of the POSA project, partly funded by the French Navy, was to pave the way for reliably assessing the risk of building damage on the adjacent shore, induced by the detonation of large-charge UXO (of between 80 and 680 kg TNT-equivalent weights) in a variable shallow water environment with a water depth less than 50-100 m. While the wave propagation generated by the detonation of small charges (usually, smaller than a few-kilograms TNT-equivalent weight) is quite well studied in the open literature (e.g., [1-3]), to the best of our knowledge, very few works are concerned with charges of a few-hundred-kilograms TNT-equivalent weight and located in coastal waters with a depth close to 50-100 m (e.g., [4-7]). In that respect, the POSA project can be considered as a pioneer work.

To understand how the seabed (and possibly, the viscoelastic sedimentary layer with a varying thickness) and the water column (with a varying depth) influence the propagation of the seismo-acoustic waves that are generated by the UXO detonation and that reach the coast, we have relied on a multidisciplinary cross-study including real data obtained within the framework of controlled countermining campaigns, and numerical simulations of the seismo-acoustic propagation using a spectral-element method. The countermining campaigns were conducted in December 2018 in the Mediterranean Sea in the Rade d'Hyères (south-eastern part of France). The real data have been collected by acoustic recording systems (namely, two hydrophones and one shock gauge) and by a relatively dense array of seismic stations (velocimeters, conventional accelerometers, and MicroElectroMechanical Systems (MEMS) accelerometers) located on the shore at a maximum of 15 km from the underwater explosion locations. Most of the results obtained from the analysis of the real acoustic and seismic data and from the numerical simulations are reported in a two-companion paper [8,9] and in a paper currently under review [10].

The present extended abstract summarizes some of the main results of the POSA project. Section 2 briefly describes the POSA experiment conducted in the Rade d'Hyères in December 2018. We refer the reader to [8,9] for further details. Section 3 then presents some of the acoustic and seismic explosion-induced signals collected by the acoustic and seismic recording systems, and also discusses the impact of the charge characteristics on the recorded signals, as well as the impact of the location of the explosion (on the seabed *vs.* in the water column). Finally, Section 4 investigates the influence of the environment geology on the seismic explosion-induced signals recorded on the shore.

2. THE POSA EXPERIMENT

2.1 Characteristics of the experiment site

The Rade d'Hyères is approximately 15 km long in the E/W direction and 10 km wide in the N/S direction. The water depth within the bay is less than 70 m (Fig.1a) and the sound speed in water was assumed constant and equal to 1507 m/s. The seabed, whose physical and geometrical properties vary laterally, is composed of unconsolidated sediments lying over a bedrock. The sedimentary cover is generally less than 5 m thick within the bay, but locally reaches 30 m close to the western part of the shore (Fig.1b). Except close to this deep sedimentary basin, the sediment properties are globally constant within the bay: measured density ρ_{sed} = 1550-2000 kg/m^3, measured P-wave velocity V_{Psed} = 1625-1750 m/s, measured P-wave attenuation α_{Psed} = 0.49-0.69 dB/m/kHz, estimated S-wave velocity $V_{Ssed} \approx$ 200 m/s, estimated S-wave attenuation α_{Ssed} = 40 dB/m/kHz. Depending on the nature of rocks, the density, P- and S-wave velocities in the bedrock vary within the bay: measured density ρ_{rock} = 2600-2650 kg/m^3, measured P-wave velocity V_{Prock} = 4100-4450 m/s, measured S-wave velocity V_{Srock} = 2700-2910 m/s. In the absence of information on their variation with depth, the rock properties were assumed to be constant with depth.

2.2 Characteristics of the detonated charges

Eight explosive charges of TNT-equivalent weights ranging from 80 to 680 kg were detonated at two specific locations in the bay (labeled 3TY and 3TZ, respectively, in Fig.1). The first seven (S1-

S7) charges were placed on the sea bottom, while the last one (S8) was placed in a container in the water column at ~11m below the sea surface. The source distance from the shore ranges from 6 to 13 km. At the locations 3TY and 3TZ, the water depth was 46 m and 29 m, respectively. We refer the reader to [8] for further details.

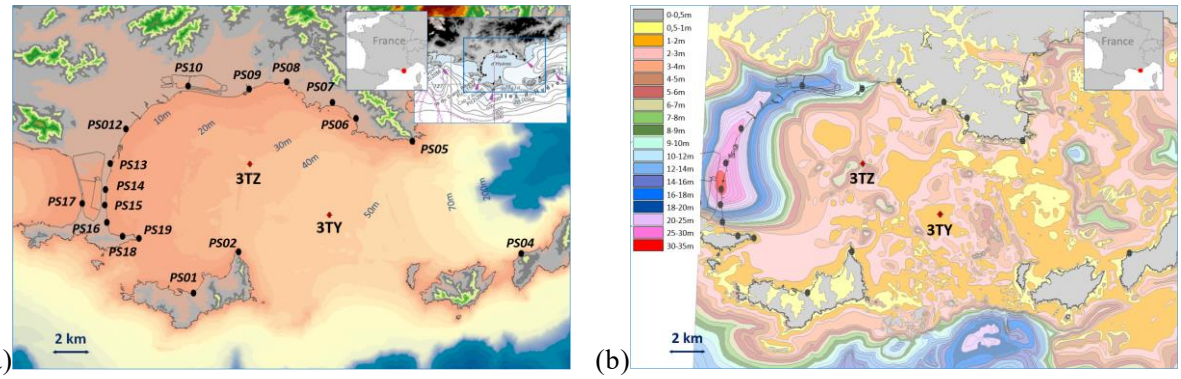

Fig.1. The experiment site, namely the Rade d'Hyères in the Mediterranean Sea (south-eastern part of France): (a) bathymetry, (b) 3D map of the sediment thickness. The two locations, labeled 3TY and 3TZ, are the locations where the UXO were detonated during the campaign of December 2018. The locations of the temporary seismological stations deployed along the shore are labeled PS01-PS19.

2.3 Hydro-acoustic and seismic experiments

The hydro-acoustic recording system consisted of a shock-gauge transducer T11-Neptune Sonar, with a nominal charge sensitivity of 0.07 pC/kPa, and two hydrophones Hi-Tech model HTI-96, with nominal sensitivities of −210 dB re 1 V/µPa (hereafter, referred to hydrophone H210) and −240 dB re 1 V/µPa (hereafter, referred to hydrophone H240), respectively. The two hydrophones have flat responses (within 3 dB) over the frequency band 0.002-30 kHz. The shock-gauge transducer was placed at a water depth of ~10 m below the sea surface and at fairly close horizontal distances (~110-270 m) from the explosive charge locations, whereas the two hydrophones were suspended at a water depth of ~10 m and at distances equal to ~ 400 or 2800 m and ~ 3000 or 5900 m from the shot locations, respectively. We refer the reader to [8] for further details.

The shock-transducer signals were recorded continuously, and the signal digitization occurred at a sampling rate of 625 kHz, giving a time resolution of 1.6 µs. As the maximum pressure level that was recorded during the experiments was around 1 MPa, *i.e.* well below the limit of the measurement system, there was no clipping. The hydrophone signals were recorded continuously, and the signal digitization occurred at a sampling rate of 78.125 kHz, giving a time resolution of 12.8 µs. The limit of the whole measurement system was 6.68 kPa for the hydrophone H210 and 214.5 kPa for the hydrophone H240. We refer the reader to [8] for further details.

A temporary seismic network consisting of 20 three-component medium to broadband velocimeters and accelerometers was deployed all along the shore on 17 sites at distances ranging from 6 to 13 km from the explosion locations (Fig.1a). The seismological stations recorded continuously during their installation period, including the seismic ground motion generated by explosions. The seismic signals were recorded with sampling rates of 250 samples per second (sps) (velocimeters) and 500 sps (accelerometers), respectively, and then band-pass filtered between 0.1 and 45 Hz (for 250 sps signals) or between 0.1 and 110 Hz (for 500 sps signals). We refer the reader to [8] for further details.

One of the originalities of the POSA experiment is the use of eight MEMS (MicroElectroMechanical Systems) accelerometers (Sercel DSU3-SA) in complement to the conventional velocimeters and accelerometers. Besides their low cost, these instruments have the great advantage of being easily installed in remote locations without external power sources. Two of the eight MEMS accelerometers were collocated with conventional seismic stations at the rocky site PS05 and at the sandy site PS13 (Fig.1a).

3. ACOUSTIC AND SEISMIC EXPLOSION-INDUCED SIGNALS

3.1 Acoustic signals

Time-series data generated by the explosion of a charge of 80 kg TNT-equivalent and recorded by

the shock gauge transducer T11 are shown at different time scales in Fig.2. The signal associated with the shock wave highlights the typical feature of a shock waveform, namely an instantaneous pressure rise (with a peak pressure at 0.15 s) followed by an exponential pressure decay (Fig.2c). The first bubble pulse arrives ~ 0.30 s after the primary shock arrival (Fig.2a), which is consistent with empirical predictions [1]. The signal arriving at ~ 0.152 s (Figs.2b and 2c) is associated with the waves reflected by the free sea surface and received before the completion of the bubble pulse from the direct wave. The signal associated with the shock wave generated by the explosions on the seabed has the same waveform, whatever the TNT-equivalent charge weight [8]. However, the shock waveform is very different for the case of an explosive charge located in the water column, namely, the exponential pressure decay following the pressure rise is largely missing because of a so-called « cut-off » (i.e. a fast pressure drop), which is consistent with the results reported in literature (see discussion in [8]).

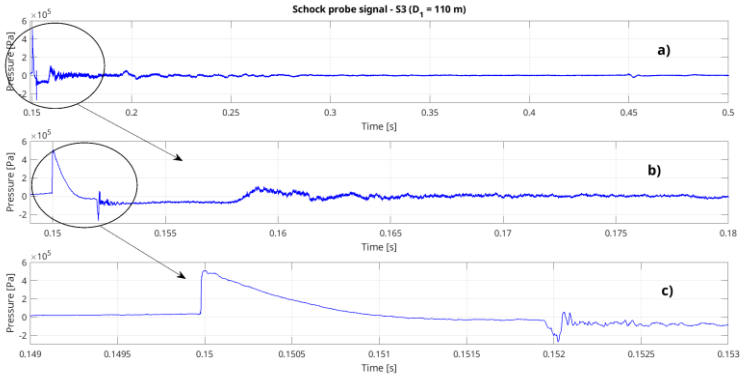

Fig.2. Signal generated by the explosion of a 80 kg TNT-equivalent charge on the seabed at 3TY, and recorded by the shock gauge transducer T11 located at 110 m from the source. Because of pyrotechnic delay, time 0.15 s cannot be considered as a reliable arrival time of the shock wave after detonation.

Time-series data generated by the explosion of a charge of 80 kg TNT-equivalent and recorded by the two hydrophones H240 and H210 are provided in Fig.3. The signal associated with the shock wave arrives at ~ 0.15 s. The first bubble pulse arrives ~ 0.30 s after this primary shock arrival on the two signals recorded by the two hydrophones. The complexity of the longer range signal recorded by the hydrophone H210, compared to the shorter range signal received at the hydrophone H240, is due to effects of the shallow water environment on the wave propagation, mainly waveguide dispersion. For the sake of brevity of this expanded abstract, we choose not to present all the signals recorded by the hydrophones, since the signals have similar waveforms for similar detonation conditions, *i.e.* for similar charge weights and for similar shallow water environments. Nevertheless, the signal waveforms depend on the charge location at a same experiment site. The signals associated with the bubble pulse have globally higher amplitudes when the charge is located in a container in the water column, rather than on the seabed, even if the charge detonated in water is of smaller weight. For further details, we refer the reader to [8].

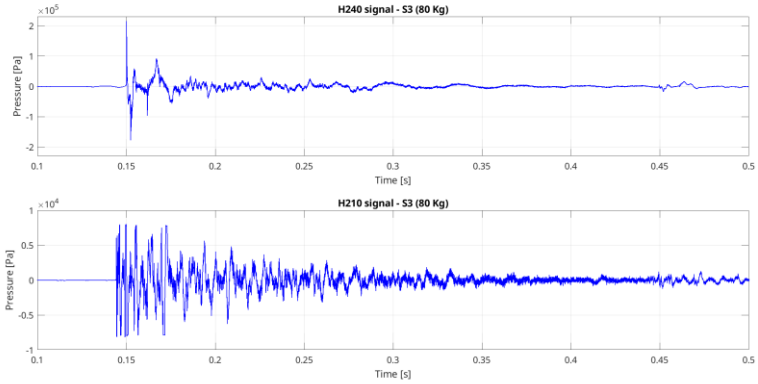

Fig.3. Signals generated by the explosion S3 (80 kg TNT-equivalent charge) located on the seabed at the location 3TY, and recorded by the two hydrophones H240 and H210 located at 326 m and 2983 m, respectively, from the source. For a better comparison, both signals are blocked on the same arrival time for the shock wave. Note also that the beginning of the shock wave signal (highest amplitude) recorded by the hydrophone H210 is slightly clipped.

Spectral analysis was carried out through the estimation of the Power Spectral Density (PSD) for the signals recorded by the shock gauge transducer T11 and the hydrophone H240. For the sake of brevity of this expanded abstract, we choose not to present the different spectra and we refer the reader to [8] for details and figures. Nevertheless, we summarize here the main key points:

i. The signal spectra are consistent for a given charge detonated at the same location (3TZ or 3TY, Fig.1a).
ii. Whatever the charge weight and wherever the explosion location, the spectra of the signals recorded by the shock transducer (located « close » to the explosion) are quite similar and relatively constant below 300 Hz. Above 300 Hz, the spectra exhibit a significant drop.
iii. Whatever the charge weight and wherever the explosion location, the hydrophone, although having a good sensitivity at low frequencies (LF), could hardly record the components with frequencies below 30 Hz, because of the waveguide cutoff frequencies.
iv. A detonation on the seabed generates lower frequencies (globally, up to 30 Hz) than a charge detonation in the water column.
v. The shock wave signal mostly contributes to the HF components of the whole spectrum (frequencies above 100 Hz), whereas the first bubble pulse signal contributes to the LF part (below 100 Hz with a peak around 30 Hz), which is consistent with information reported in literature (see discussion in [8]). Because of its contribution to the lower frequency part, the bubble pulse signal may be the most appropriate candidate to possibly generate seismic risks, in particular in the presence of sedimentary basins. Indeed, the sedimentary basins may lower the frequency content of the signals while locally amplifying their amplitude. This is the well-known site effect observed in seismology, that can damage the buildings.

3.2 Seismic signals

For the sake of brevity of this expanded abstract, we choose not to present all the seismic signals and we refer the reader to [8,10] for details. Nevertheless, in order to show the impact of the weight and the location of the explosive charges on the seismic signals arriving at the shore, we compare the vertical component of the ground acceleration induced by each explosion (S1-S8) and recorded at the same station PS05 (Fig.4a). Firstly, for a given location for explosions (3TY or 3TZ) and for similar conditions (*i.e.* located on the seafloor), the signals are consistent. Secondly, the ground acceleration is linearly related to the charge weight.

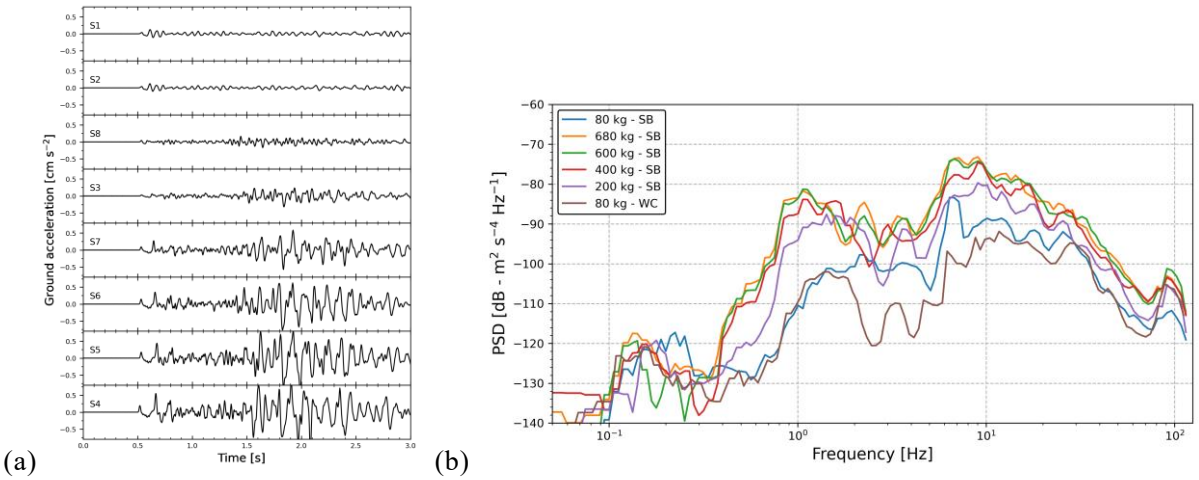

(a) (b)

Fig.4. (a) Vertical component of the ground acceleration, generated by the explosions S1-S8, and recorded by the velocimeters at the station PS05 (see Fig.1). S1 and S2 correspond to a 80 kg TNT-equivalent charge located at the site 3TZ, S8 to a 80 kg TNT-equivalent charge located at 3TY in the water column (WC), and S3, S7, S6, S5, S4 to a 80, 200, 400, 600, 680 kg TNT-equivalent charge, respectively, located at 3TY on the seabed (SB). The amplitudes are graphically clipped between ±8 mm.s^{-2} for clarity of display. (b) Power spectral densities (PSD) of the vertical ground-acceleration components induced by the explosions S3-S8.

Spectral analysis shows that the detonation of charges of weight larger than 80 kg TNT-equivalent generates globally similar spectral responses for the vertical ground-acceleration components recorded on the shoreline (Fig.4b). However, the amplitudes of the spectral responses increase with increasing charge weight. Whatever the source, the most energetic peak at ~ 10 Hz is likely associated

with bulk wave propagation. The secondary peak observed in the 0.8-2 Hz frequency range, but only for the largest charges, is likely associated with interface/surface wave propagation.

Compared to a charge detonation in the water column, a similar detonation on the seabed generates seismic signals of much lower frequencies (< 30 Hz) and higher amplitudes that propagate in the seabed (see *e.g.* the signals generated by the explosions S3 and S8, both corresponding to a 80 kg TNT-equivalent charge, and the associated spectra in Fig.4), Detonating the charges directly on the seafloor, and not close to, makes the coupling between the source and the seafloor super-efficient [11].

Two empirical laws for the explosion-induced local seismic magnitude, as a function of the charge weight, have been derived in [8] for the cases of a charge detonation in the water column and on the seabed, respectively. These two laws globally follow the same trend, but with a shift of 0.5 in magnitude, since much less energy is transmitted downwards into the ground when the explosion takes place at a shallow water depth. Note that, in the POSA experiment, the charge detonations (up to 680 kg TNT-equivalent) have generated seismic events of at most magnitude 2.9 on the Richter scale.

It is worth noting that the contribution of phases, that are not recorded by conventional sensors at usual sampling rates (*i.e.* less than 250 sps), could be observed from the high sampling rate data (500 sps) recorded by the MEMS accelerometers. Besides the P and S waves, and the interface/surface waves that follow them, a high-frequency high-amplitude signal with a velocity close to the sound speed in water could also be observed at some stations located on rocky sites with a thin sedimentary cover [10]. This signal likely corresponds to a H-phase (following the IASPEI nomenclature), *i.e.* a wavepacket that propagates within the water column from the source to a location close to the shore (at the cutoff height of the acoustic modes) and that subsequently converts to seismic energy before being recorded by the seismic sensor. In addition, at some seismic stations, an energy packet with an apparent velocity close to the sound velocity in the air could also be observed when the largest charges were detonated on the seabed [10]. This is likely an I-phase (following the IASPEI nomenclature), *i.e.* an acoustic phase that propagates in the air from the explosion location.

4. INFLUENCE OF THE ENVIRONMENT GEOLOGY ON THE SEISMIC SIGNALS

Fig.5. illustrates the seismic ground motion induced by the detonation of a 400 kg TNT-eq. charge (S6) located on the seabed at the site 3TY and recorded by the network of 20 three-component (3C) velocimeters and accelerometers deployed all along the shore of the Rade d'Hyères (Fig.1a).

The global signal waveforms and durations greatly differ according to the explosion-station distance, and according to the ground properties along the propagation path as well. The sediment thickness seems to have a significant influence, since for the stations PS09-PS17 installed on sites with several meters of sediments below, the first P-wave arrival is not as impulsive as the one observed at the other sites. Most importantly, the signal duration is much longer, with the presence of late dispersive signals with a very LF content and, for some stations, large amplitude. The largest amplitudes are generally observed for S waves and surface waves, with amplifications that can be significant on the horizontal components (*e.g.*, stations PS10 and PS17). These characteristics are specific to the well-known site effects induced by the sedimentary basin [10], and can be well explained and illustrated by full-wave numerical simulations of wave propagation [9]. For the sake of illustration, Fig.6 shows how the different types of waves (namely, P and S waves, interface and surface waves of Stoneley-Scholte (SS), and Rayleigh or Rayleigh-Sezawa (Rayl) type) interact with the physical properties and the geometry of the marine environment (including the laterally-varying sedimentary layer), and how they evolve along the propagation path between the explosion location and the station location. However, from Fig.5 no strong conclusion can be drawn from the observed differences in the signal amplitudes. Indeed, several factors, including the source-station distance and the conditions of the station set-up on the rocky or sedimentary sites, may also impact the wave amplitudes.

In [10] we further investigate the importance of the sedimentary cover on the frequency content of the seismic signal recorded at the shore. The thick sediment layer is shown to generate important seismic amplifications (H/V ratio up to 20) of the relatively low-frequency energy (1 to 5 Hz). In [10] we evidence that the sedimentary cover has to be taken into account to mitigate potential nuisance on land for large charge weights in shallow water environments.

It is worth noting that, although the largest charge (680 kg TNT-eq.) detonation on the seabed generated a seismic event of magnitude 2.9 on the Richter scale, no infrastructure located on the shore of the Rade d'Hyères was damaged. For the sake of illustration of the seismic response on nearby civil engineering structures, two velocimeters were located at the top and the bottom (station PS01),

respectively, of the bell tower of the Ste-Anne church located on the Porquerolles Island (Fig.1a). During the POSA experiment, this masonry structure faced motion amplification in response to the explosion-induced seismic signal, but that deformation was well beyond the damage initiation threshold [8,10].

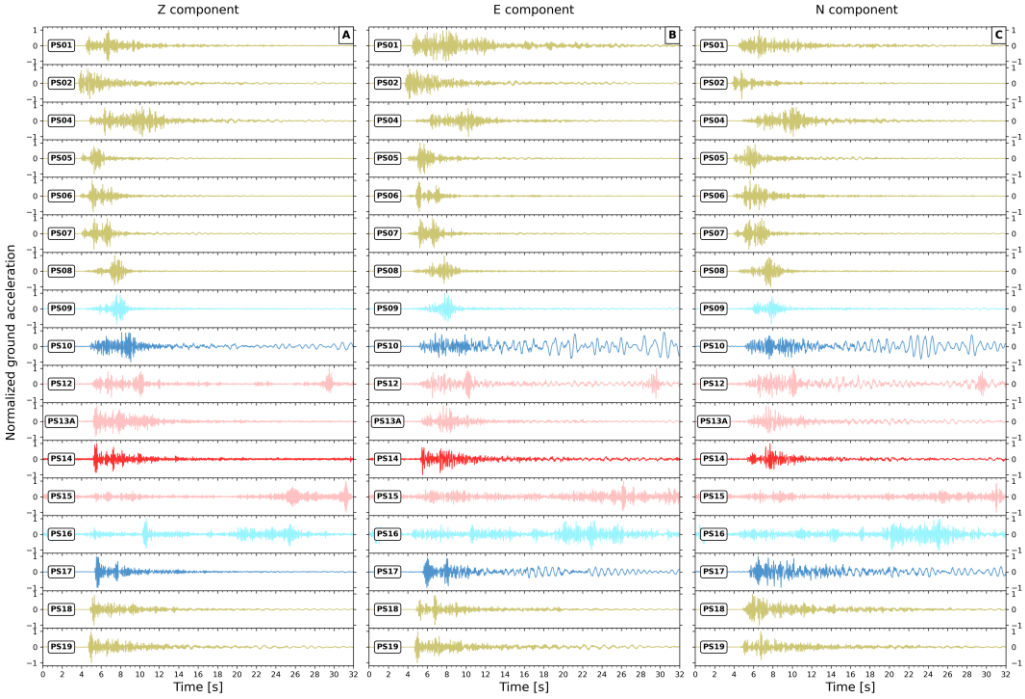

Fig.5. 3C ground accelerations (GA) induced by the explosion of a 400 kg TNT-eq. charge located at 3TY and recorded at PS01-PS19 (Fig.1a). Each signal amplitude is normalized by the maximum amplitude of the corresponding GA. The signals are low-pass filtered at 20 Hz. All the traces are plotted with the same origin time, and the amplitudes are graphically clipped between ± 5 mm.s^{-2} for display clarity. Sandy color: sites with a thin sedimentary layer (0-1 m), red-pink and blue colors: sites with a thick one (see Fig.1b).

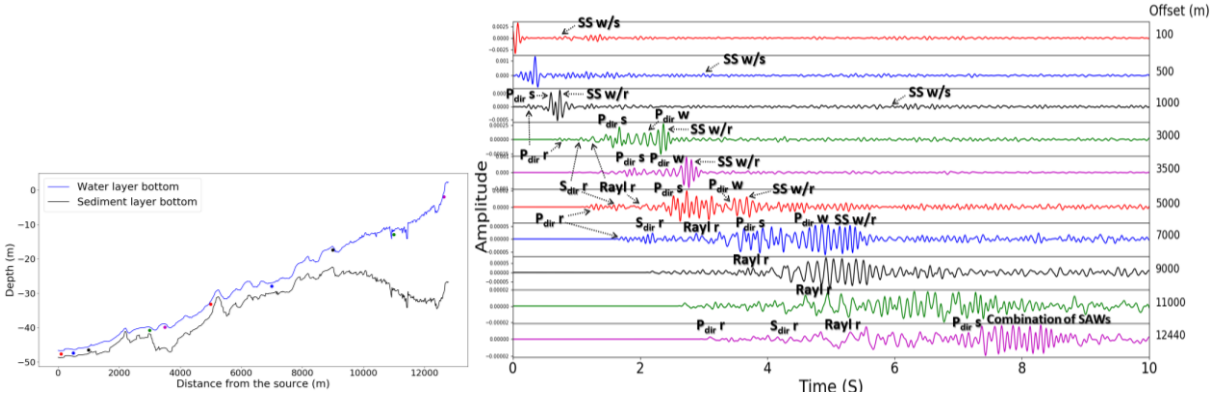

Fig.6. (Left) Bathymetry, geometry of the sedimentary layer, and location of the fictitious horizontal receiver array (colored dots) along the line 3TY-PS13. (Right) Focus on the first 10 s of the simulated seismograms related to the horizontal component of the velocity. For the sake of a better visualization, the signals obtained at the different offsets are represented at different amplitude scales. See [9] for the explanations of the different labels related to the different kind of waves. The numerical simulations were performed using a spectral-element method.

5. CONCLUSION

This expanded abstract summarizes some of the main results related to recorded acoustic and seismic signals induced by the detonation of large charges (with weights up to 680 kg TNT-eq.) in the framework of a UXO countermining campaign conducted in a variable shallow water environment, namely the Rade d'Hyères in the Mediterranean Sea (France) in December 2018 (POSA project). As expected, the acoustic and seismic signal amplitudes increase with increasing charge weight. A

detonation on the seabed generates lower frequencies (globally, up to 30 Hz) than a charge detonation in the water column. The variable environment characteristics, in terms of bathymetry, thickness of the sedimentary layer, and physical properties, have a significant influence on the complex wave propagation towards the shore and on the acoustic-to-seismic conversions. In particular, the presence of sedimentary basins can induce site effects, *i.e.* large amplification of the S-wave and interface/surface-wave amplitudes, increase in the signal duration and shift of the spectrum towards the very low frequencies.

ACKNOWLEDGEMENTS

This work was supported in part by The French National Research Agency (ANR) and in part by the DGA (French Ministry of Defense Procurement Agency) under Grant ANR-15-ASTR-0001 POSA.

This work was granted access to the seismic resources of Résif-EPOS that is a Research Infrastructure (IR) managed by CNRS-Insu. Inscribed on the roadmap of the Ministry of Higher Education, Research and Innovation, the Résif-EPOS IR is a consortium of eighteen French research organizations and institutions. Résif-EPOS benefits from the support of the Ministry of Ecological Transition. Data from the POSA experiment are distributed through the Résif-EPOS webservices (https://seismology.resif.fr) under the network code ZH (Deschamps A. and Beucler E., POSA experiment. RESIF - Réseau Sismologique et géodésique Français, 2013).

This work was also granted access to the French HPC resources of TGCC under allocation gen 7165 and mam0305 and of CINES under allocationA0020407165 andA0030410305, both made by GENCI, and of the Aix-Marseille Supercomputing Mesocenter under allocations h025.

The authors greatly acknowledge the Préfecture de la Méditerranée, the Groupe des Plongeurs Démineurs and the Force de Guerre des Mines for their management of the countermining operations. X. Mathias, P. Guyomard, E. Brenon, H. Gauduin, M. Gosselin, J.-P. Boivin, and F. Jourdin (Shom/GHOA) are acknowledged for the hydrographic and geological surveys. Semantic-TS and P. Bernardi are acknowledged for their help with the acoustic surveys. X. Martin and J. Chèze (Géoazur), Ph. Langlaude and M. Pernoud (Cerema), and M. Perrault (Cerema, now at Sercel S.A.) are also acknowledged for their help with the seismic surveys.

REFERENCES

1. Chapman, NR. Measurement of the waveform parameters of shallow explosive charges. J Acoust Soc Am. 1985;78(2):672-681.
2. Nolet G., Dorman LM. Waveform analysis of Scholte modes in ocean sediment layers. Geophys J Int. 1996; 125:385-396.
3. Soloway AG., Dahl PH. Peak sound pressure and sound exposure level from underwater explosions in shallow water. J Acoust Soc Am. 2014; 136(3):EL218–EL223.
4. Hunter KS., Geers TL. Pressure and velocity fields produced by an underwater explosion. J Acoust Soc Am. 2004;115(4):1483-1496.
5. von Benda-Beckmann AM. *et al.* Assessing the impact of underwater clearance of unexploded ordnance on harbour porpoises (Phocoena phocoena) in the Southern North Sea. Aquat Mamm. 2015;41(4):503-523.
6. Gitterman Y., Sadwin LD. Blast wave observations for large-scale underwater explosions in the Dead Sea. In: Ben-Dor G., Sadot O., Igra O. editors. 30th International Symposium on Shock Waves 2. Springer International Publishing; 2017. p. 1315-1319.
7. Salomons EM. *et al.* Noise of underwater explosions in the North Sea. A comparison of experimental data and model predictions. J Acoust Soc Am. 2021; 149(3):1878-1888.
8. Favretto-Cristini N. *et al.* Assessment of risks induced by counter-mining unexploded large-charge historical ordnance in a shallow water environment: Part 1. Real case study. IEEE J Ocean Eng. 2022; 47(2): 350-373.
9. Favretto-Cristini N. *et al.* Assessment of risks induced by counter-mining unexploded large-charge historical ordnance in a shallow water environment: Part 2. Modeling of seismo-acoustic wave propagation. IEEE J Ocean Eng. 2022; 47(2): 374-398.
10. Bonnin M. *et al.* Short range recordings of shallow underwater explosions with short period and broad-band seismometers in the Bay of Hyères, France. Submitted to Bull Seismol Soc Am. 2022
11. Garlan T. *et al.* Circular sedimentary figures of anthropic origin in a sediment stability context. J Coast Res 2018; SI 85:411-415.